LLNL-JRNL-463743

LAWRENCE LIVERMORE NATIONAL LABORATORY

A diamond detector for inertial confinement fusion X-ray bang-time measurements at the National Ignition Facility

A. G. MacPhee, C. Brown, S. Burns, J. Celeste, S. H. Glenzer, D. Hey, O. S. Jones, O. Landen, A. J. Mackinnon, N. Meezan, J. Parker, D. Edgell, V. Y. Glebov, J. Kilkenny, J. Kimbrough

December 8, 2010

Journal of Instrumentation

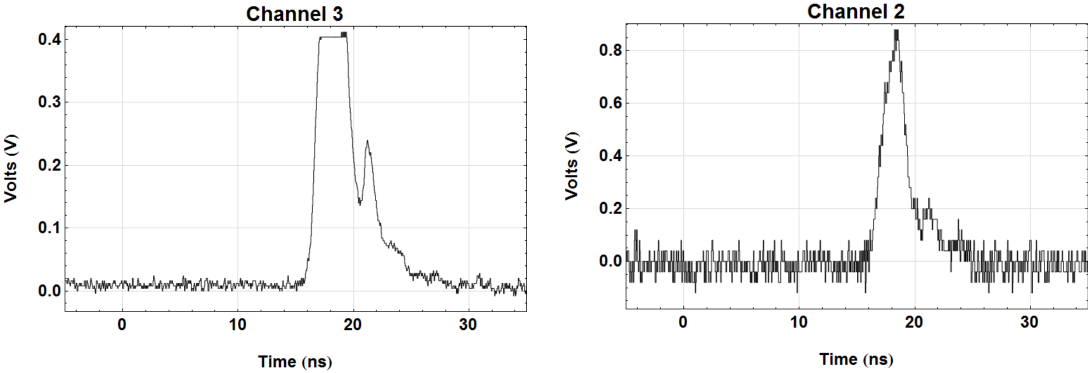

Channel 3
Volts (V)
Time (ns)
0.4
0.3
0.2
0.1
0.0
0
10
20
30
Channel 2
Volts (V)
Time (ns)
0.8
0.6
0.4
0.2
0.0
0
10
20
30

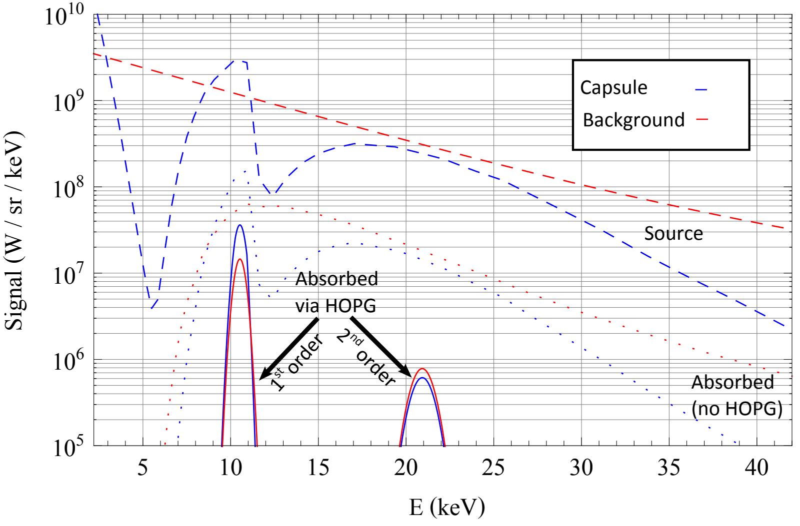

Signal (W / sr / keV)
E (keV)
10^{10}
10^{9}
10^{8}
10^{7}
10^{6}
10^{5}
5
10
15
20
25
30
35
40
Capsule
Background
Source
Absorbed
via HOPG
1st order
2nd order
Absorbed
(no HOPG)

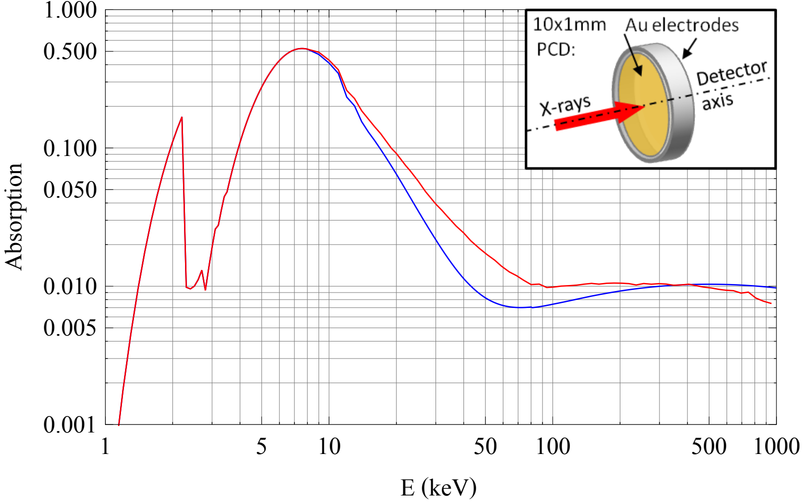

1.000
0.500
0.100
0.050
0.010
0.005
0.001
Absorption
1
5
10
50
100
500
1000
E (keV)
10x1mm
PCD:
Au electrodes
Detector
axis
X-rays

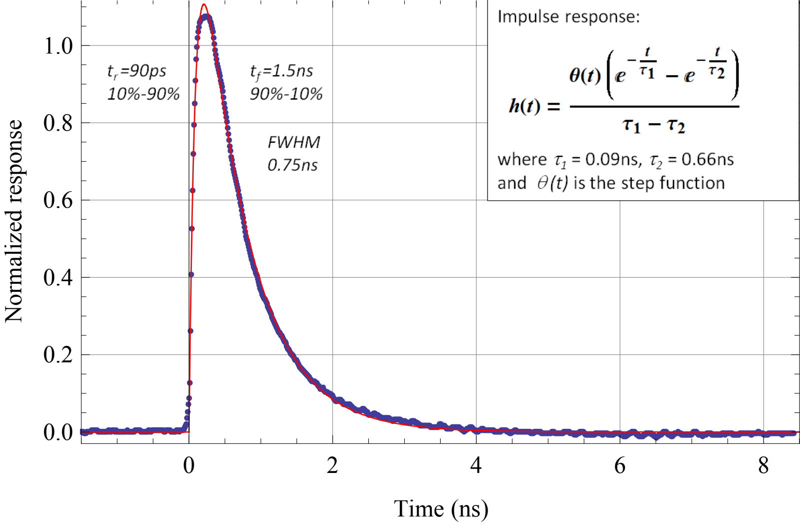

Impulse response:
$$h(t) = \frac{\theta(t)\left(e^{-\frac{t}{\tau_1}} - e^{-\frac{t}{\tau_2}}\right)}{\tau_1 - \tau_2}$$
where τ_1 = 0.09ns, τ_2 = 0.66ns
and $\theta(t)$ is the step function
t_r=90ps
10%-90%
t_f=1.5ns
90%-10%
FWHM
0.75ns
Normalized response
Time (ns)
0.0
0.2
0.4
0.6
0.8
1.0
0
2
4
6
8

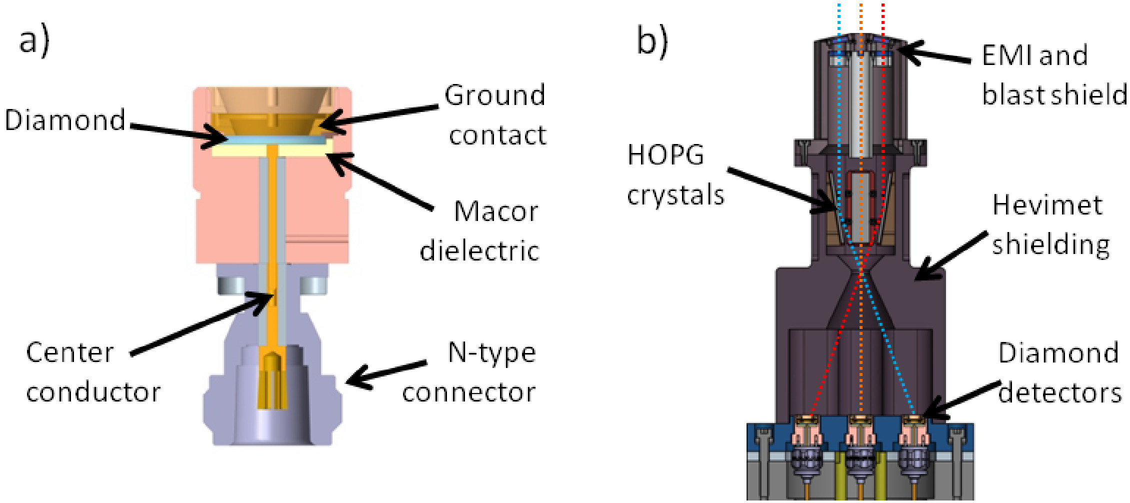
a)
Diamond
Ground contact
Macor dielectric
Center conductor
N-type connector
b)
EMI and blast shield
HOPG crystals
Hevimet shielding
Diamond detectors

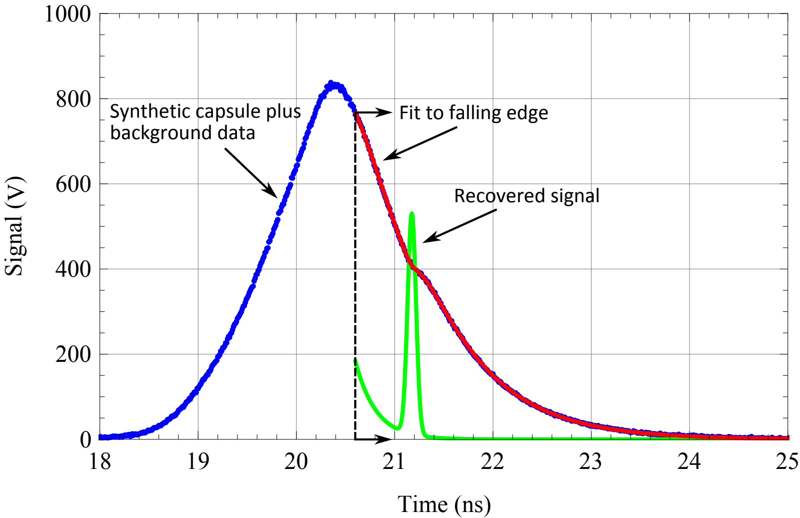

Synthetic capsule plus background data
Fit to falling edge
Recovered signal
Signal (V)
Time (ns)
1000
800
600
400
200
0
18
19
20
21
22
23
24
25

A diamond detector for X-ray bang-time measurement at the National Ignition Facility

Andrew G. MacPhee[a1], Dana H. Edgell[b], Essex J. Bond[a], Charles G. Brown[a], Scott R. Burns[a], John R. Celeste[a], Charles J. Cerjan[a], Mark J. Eckart[a], Vladimir Y. Glebov[b], Siegfried H. Glenzer[a], Daniel S. Hey[a], Ogden S. Jones[a], Joseph D. Kilkenny[c], Joseph R. Kimbrough[a], Otto L. Landen[a], Andrew J. Mackinnon[a], Nathan B. Meezan[a], Jacob M. Parker[a], Ryan M. Sweeney[a]

[a] *Lawrence Livermore National Laboratory,*
7000 East Ave., Livermore, CA 94550, USA

[b] *University of Rochester, Laboratory for Laser Energetics,*
250 E. River Rd., Rochester, NY 14623 , USA

[c] *General Atomics,*
3550 General Atomics Court
San Diego, CA 92121, USA

E-mail: macphee2@llnl.gov

ABSTRACT: An instrument has been developed to measure X-ray bang-time for inertial confinement fusion capsules; the time interval between the start of the laser pulse and peak X-ray emission from the fuel core. The instrument comprises chemical vapor deposited polycrystalline diamond photoconductive X-ray detectors with highly ordered pyrolytic graphite X-ray monochromator crystals at the input. Capsule bang-time can be measured in the presence of relatively high thermal and hard X-ray background components due to the selective band pass of the crystals combined with direct and indirect X-ray shielding of the detector elements. A five channel system is being commissioned at the National Ignition Facility at Lawrence Livermore National Laboratory for implosion optimization measurements as part of the National Ignition Campaign. Characteristics of the instrument have been measured demonstrating that X-ray bang-time can be measured with ±30ps precision, characterizing the soft X-ray drive to +/- 1eV or 1.5%.

KEYWORDS: Inertial confinement fusion; photoconductive detector; polycrystalline diamond; X-ray bang-time.

[1] Corresponding author.

Contents

1. Introduction

Efficient, isotropic coupling of hohlraum X-rays to the ablator of an inertial confinement fusion (ICF) fuel capsule are key to optimizing implosions for the National Ignition Campaign (NIC) at the National Ignition Facility (NIF) at the Lawrence Livermore National Laboratory (LLNL) [1]. Comparisons between the measured peak X-ray emission, or X-ray "bang time" and the predicted peak X-ray emission from radiation-hydrodynamic simulations [2,3] are important to tune the drive parameters to optimize the implosion [4,5].

X-ray streak cameras and framing cameras possess sufficient temporal resolution to resolve X-ray bang time, however above ~10^{14} neutron yield these instruments are increasingly susceptible to neutron background, principally because the time resolved data is converted to an two dimensional image that is recorded with neutron sensitive components in close proximity to the source. In addition due to instrument jitter and absolute timing uncertainty, X-ray bang-time measured with framing cameras cannot be guaranteed to the +/-30ps precision required for accurate comparison with neutron bang times and modelling [4]. To eliminate these limitations for higher yield shots, a photoconductive detector (PCD) originally designed to measure neutron bang-time on capsule implosion experiments [6,7] was adapted to record broadband X-ray data during the NIC energetics campaign in 2009 [8]. This was achieved by reducing the filter to 1mm Kapton and 20µm Ti. The PCD was a 5mm diameter 250µm thick chemical vapour deposited polycrystalline diamond operating at -200V bias. In this configuration the device was sensitive to X-rays above ~5keV. The device was attached to the side of a multi pinhole array gated X-ray imager mounted in the NIF polar diagnostic instrument manipulator 49cm from target chamber centre (TCC). The device viewed the capsule through the hohlraum laser entrance hole (LEH) 12º from the hohlraum axis. Figure 1 show the highest contrast X-ray bang-time signal recorded using the diamond detector, corresponding to NIF shot N091030; an 840kJ, 19ns, 100% He filled 1.07 scale 300eV cryo hohlraum with a He7%D filled 185µm wall thickness CH capsule. The PCD signal was split into two 6GHz analogue bandwidth oscilloscope channels with 40ps sampling interval and full scale set at 4V and 0.4V respectively, after a total of 32dB attenuation per channel. This enabled the ~45V background pulse to be measured on channel 2 without saturating and the relatively weak ~4.5V capsule signal measured on channel 3, on the falling edge of the background. As this was the only shot for which an estimate of X-ray bang time could be made using this instrument and subsequent shots at higher energy would suffer from even higher background, we designed a new instrument to provide higher contrast described below.

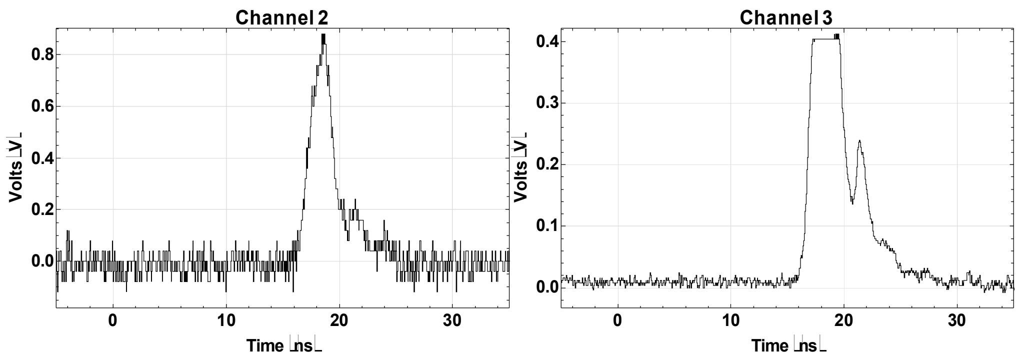

Figure 1. X-ray signal split into two oscilloscope channels at 1V/div and 0.1V/div. Both attenuated by 32dB. NIF shot N091030. 5mm diameter x 0.25mm thick diamond detector.

2. Polar view for reduced background

The X-ray bang-time signal from the capsule observed during the fall 2009 campaign was subject to significant background due to thermal radiation and laser plasma interactions (LPI) induced bremsstrahlung radiation from the inside wall of the hohlraum visible through the LEH. Although the relative brightness of these background components as a function of time has not been well characterized, it is clear that within the bandwidth of the detector both components can be significantly reduced by moving the instrument onto the hohlraum axis, as the 80µm thick gold wall surrounding the hohlraum LEH will effectively eliminate X-rays below ~30keV generated in or near the hohlraum wall. In addition the time averaged LEH transmission measured using the soft X-ray imager (SXI) [9] in the region 3-5keV on the 1MJ 10%DHe3 NIF shot N091204 suggests that the effective diameter of the LEH is reduced from 3.1mm to ~2.6mm during the shot. At bang-time the capsule diameter is reduced to ~100µm and the capsule centre of mass can shift by up to ~50µm. Viewed 12º off-axes, the line of sight from the diamond detector to TCC is within ~250µm of the inner edge of the LEH. Moving the instrument on-axis will therefore ease alignment tolerance ensuring a clear view of the capsule and simultaneously reduce bremsstrahlung and thermal background.

3. Monochromator for enhanced contrast

For symmetry tuning targets with ~2keV core temperature, peak photon energy at bang-time is ~10keV. Tritium hydrogen deuterium (THD) ignition capsules exhibit higher convergence ratio so that under similar hohlraum conditions their core temperature is ~5keV, giving peak photon energy at bang time of ~20keV. Absorption in the germanium doped ablator above the germanium K-edge at 11.1keV shifts peak emission down to ~11keV.

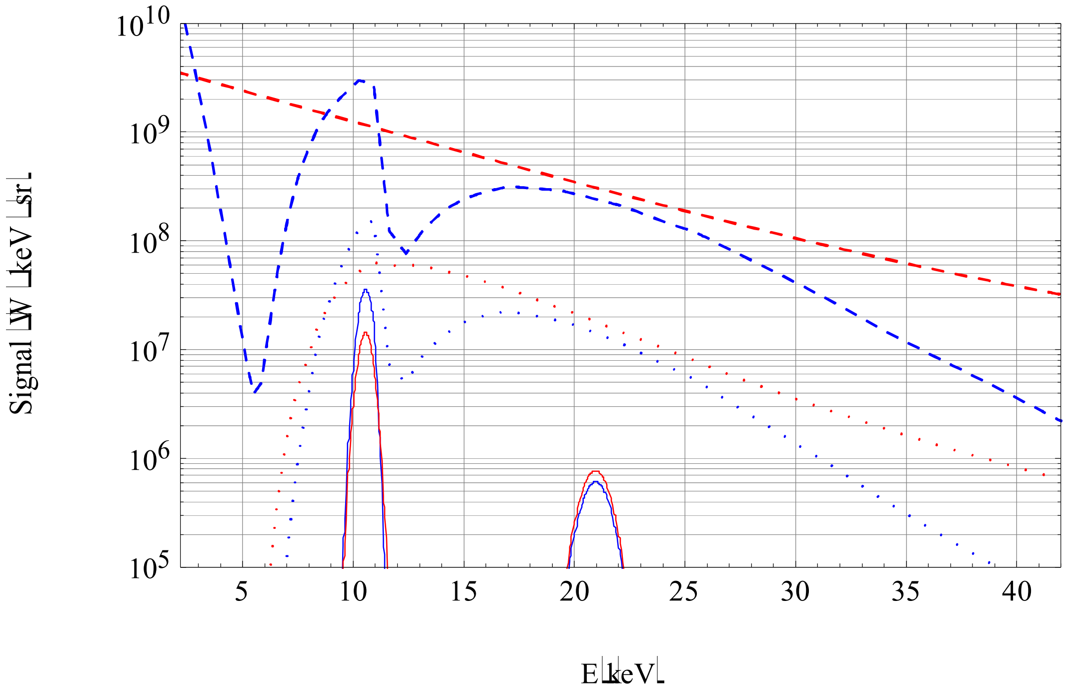

Figure 2. Signal levels for a 1MJ THD shot. Source spectra (dashed): Capsule [10] (blue), hohlraum [11] (red). Signal deposited in detector: without HOPG (dotted), with HOPG (solid). Signal via HOPG in 1st and 2nd order at 11keV and 22keV respectively

The dashed blue curve in figure 2 is the simulated on-axis capsule spectrum at bang-time for a successful 1MJ THD shot [10], produced using the radiation hydrodynamics code Lasnex [2]. The background spectrum illustrated by the dashed red curve is inferred from time integrated filtered fluorescence X-ray detector (FFLEX) data [11] measured for an equivalent shot and converted to power based on the ~2ns FWHM measured with the high energy time resolved FFLEX channel. The dotted curves represent these signals folded through the X-ray instrument response function (xIRF) for a 1mm thick diamond PCD with 1µm thick gold electrodes (figure 3) filtered with 20µm titanium and 3mm Kapton. Differentially filtered pinhole camera images of capsule implosions demonstrate that mix of Ge dopant from the shell into the hot core [12,13] produces Ge He-alpha X-ray features at 10.3keV that may bias X-ray bang-time measurements. Together these observations suggest that contrast against thermal background, bremsstrahlung and mix features will be maximized by spectrally selecting the region towards the upper end of the capsule peak between 10.5keV and 11.5keV. Capsule burn time is predicted to be of the order ~100ps [10], one twentieth of the hohlraum background duration. Consequently to maintain X-ray contrast for weak capsule signals it is also essential to minimize the temporal response of the detector.

To this end and to better constrain the spectral range reported for X-ray bang-time for comparison with modelled data when tuning hohlraum implosions, we are commissioning a new instrument, South Pole Bang-Time (SPBT) with highly ordered pyrolytic graphite (HOPG) monochromating crystals (see for example [14] and [15]) tuned for 11keV X-rays. The crystal grade chosen has 0.8º mosaicity and exhibits ~25% and ~4% peak reflectivity at 9.7º incidence angle in first order and second order with ~8% bandwidth at 11keV and 22keV respectively. This configuration enables timing the instrument using 22keV silver K_α radiation in second order reflection from the crystal generated by an 88ps impulse shot on a silver foil target. The lower dashed curves in figure 2 represent the capsule and background spectra estimated for the 1MJ THD shot folded through the xIRF including the HOPG monochromating crystal. The instrument has four monochromator channels and a single on-axis channel with a direct view of the capsule. The four monochromator channels are filtered to provide a combined dynamic range of ~10^4 without the need to break vacuum. The on-axis channel will primarily be used as a timing channel using impulse shots. This channel will also provide on-shot timing information from the LEH X-ray flash at t_0, neutron, proton and broadband X-ray timing data.

The PCD is a 1mm thick diamond disc 12mm diameter with 1µm thick, 10mm diameter gold electrodes on both sides and signal enters the diamond through one of the electrodes. Figure 3 shows the fraction of energy deposited in the diamond as a function of photon energy. The red curve is a Monte Carlo simulation (Integrated Tiger Series 3.0 (ITS 3.0) [16]). The blue curve represents the absorbed fraction based on NIST data for transmission through gold and absorption in carbon. Both curves include Compton scattering which dominates the energy deposition mechanism above ~50keV. Above the gold L-edge at ~12keV, the ITS simulation shows that energy deposited in the diamond is enhanced by secondary products, fluorescence and Compton electrons generated in the electrodes. Conversely from 100keV to 450keV the energy deposited in the diamond is reduced, as the electron range in diamond increases from 50µm to 500µm and energy transferred to electrons can escape. This detector configuration provides contrast between the capsule peak photon energy at ~11keV and the Bremsstrahlung and thermal radiation background from the hohlraum that extends for several hundred kilovolts and enables a compact, high electrical bandwidth coaxial assembly.

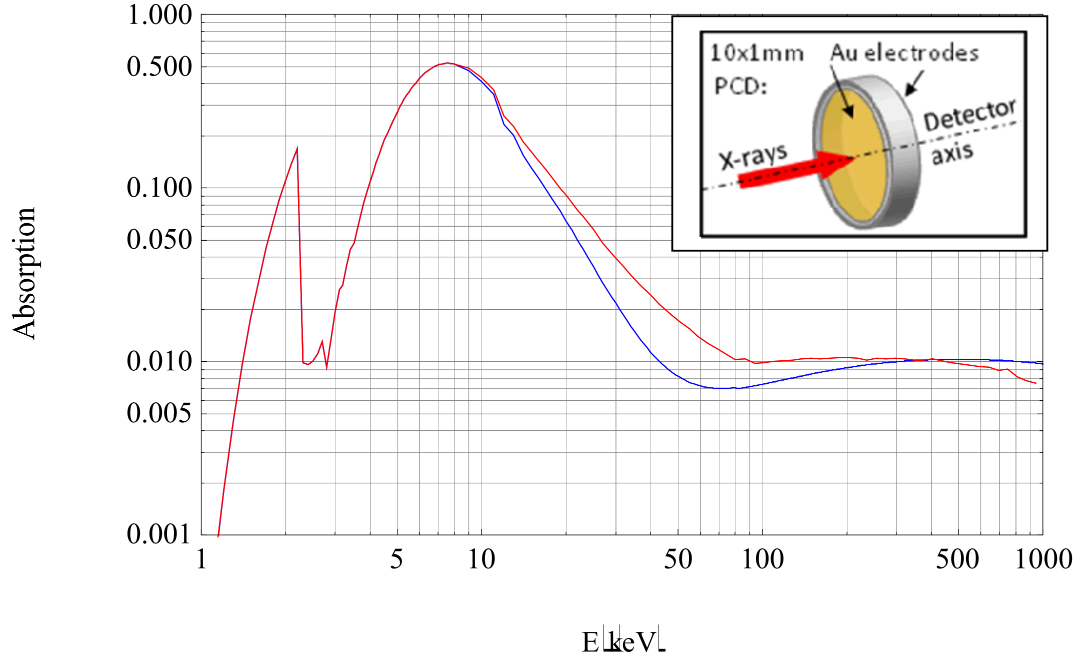

Figure 3. Energy deposited in a 1mm thick diamond PCD with 1µm thick gold electrodes. NIST transmission and absorption data (blue) Monte Carlo simulation including secondary products (red)

4. Temporal Instrument Response Function

The temporal instrument response function (tIRF) is the response of the system to an impulse. To recover X-ray bang-time and plasma burn duration from the oscilloscope trace, the data is fit to a Gaussian pulse convolved with the measured tIRF. The peak and width of the Gaussian are reported as X-ray bang-time and burn width respectively. The tIRF for the system was measured by irradiating the diamond detector with an ultra short laser produced X-ray pulse and recording the response on an oscilloscope. 5-8keV X-rays from a solid Cu target were used, filtered with a 25µm Cu foil. The target was irradiated at $>10^{16}$ W/cm^2 with a ~4J, <4ps laser pulse in an F/2.5 focusing geometry at the Comet laser, part of the Jupiter Laser Facility at LLNL. The tIRF was recorded using a fast transient digitizer (FTD10000 [17]) with 10ps sample interval, a 10ns window and 7GHz analogue bandwidth. The duration of the X-ray emission was measured using a Kentech low-magnification X-ray streak camera filtered to record >5keV X-rays. The X-ray pulse length within the dynamic range of the streak camera was at most ~6ps, limited by the temporal resolution of the instrument. The tIRF for the system is plotted in figure 4, along with a best fit comprising the convolution of two exponentials. The 10% to 90% rise and fall times are 90ps and 1.5ns respectively. The ~6ps X-ray pulse is significantly shorter than the rise time and therefore contributes little to the inferred response function.

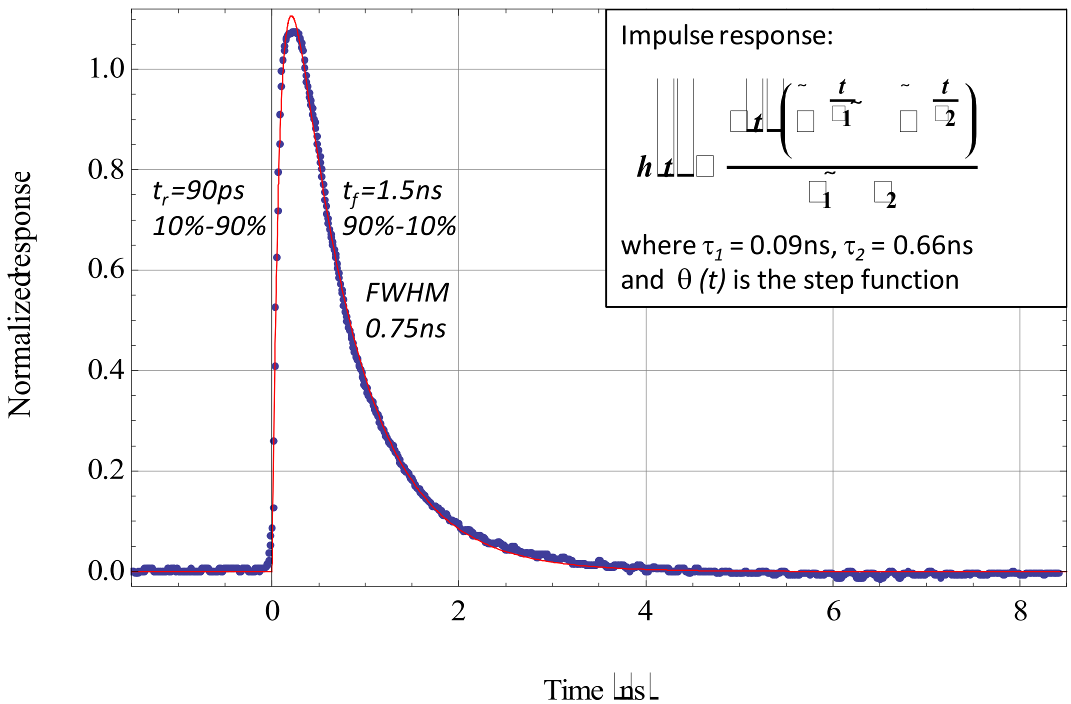

Figure 4. Temporal instrument response function recorded using a 10ps per sample 7GHz bandwidth fast transient digitizer. The best fit solid curve is a convolution of two exponentials with τ_1=0.09ns and τ_2 =0.66ns

5. Detector layout

Figures 5a and b show cross sections through the detector head and an individual diamond detector assembly based on an original design by Glebov [7]. In the current design 50Ω impedance is maintained up to the surface of the diamond where the transition from coaxial connector to diamond surface is facilitated with a Macor dielectric disc coaxial to the centre conductor also at 50Ω and a 15μm thick gold sputter coated electrode. This configuration eliminates significant ringing in the vicinity of the peak of the impulse response function.

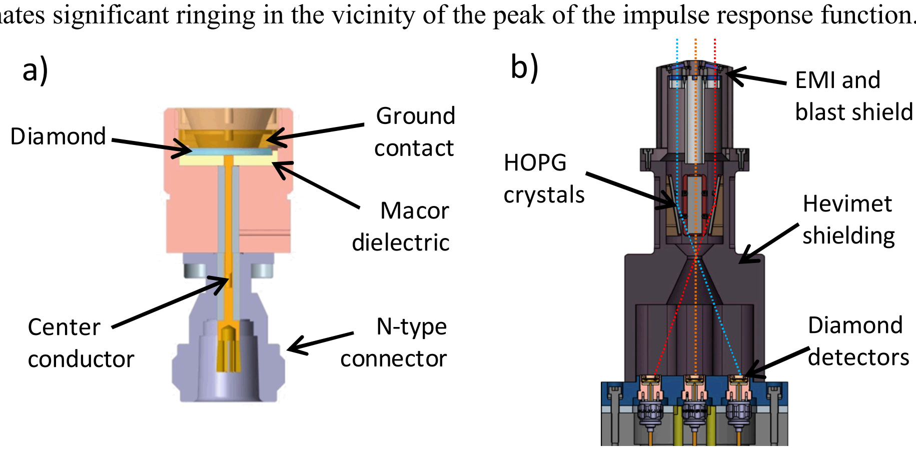

Figure 5. a) N-type diamond assembly b) complete detector head. Centre channel has direct line of sight to capsule. Four HOPG channels shielded from direct radiation by at least five centimeters of hevimet

The detector head is located on the vertical axis of the chamber 3m below TCC and supported from an off axis flange near the south pole of the chamber. The signal is brought to the chamber wall via >20GHz bandwidth semi rigid cable with >165dB shielding effectiveness.

6. Data reduction

Simulations suggest that hohlraum background falls rapidly after the laser pulse switches off [18]. This correlates with the observed broad band diamond detector traces from the fall 2009 campaign where the exponential fall matched the estimated fall time of the instrument. Simulations of the imploding capsule for THD and DT target configurations with varying degrees of symmetry [10,18] also suggest that burn duration remains approximately constant at ~100ps with an approximately Gaussian shape. X-ray bang-time and burn duration can therefore be retrieved from south-pole bang-time oscilloscope trace data by fitting it to a falling exponential plus a Gaussian, convolved with the temporal instrument response function. The green curve in figure 6 is the X-ray temporal profile recovered using such a fit (red curve) to a simulation where EMI noise and oscilloscope quantization have been included (blue data points). The data range used for the fit starts on the falling edge of the hohlraum background at t=20.6ns and continues to the end of the record. The accuracy of the fit is strongly dependent on the contrast between capsule emission and hohlraum background. For the simulation in figure 6, representing an unturned THD implosion [18] where X-ray contrast is as low as we expect, a ±13ps shift in the peak from best fit gives a 1σ increase in the standard deviation from the data. Combined with the estimated error in the on-shot timing fiducial (±8ps) and the absolute definition of t_0 based on an X-ray impulse shot (±10ps) also measured relative to a timing fiducial, it is estimated that the overall uncertainty in X-ray bang-timed measured with this instrument will be in the vicinity $\pm((13^2+8^2)^{0.5} + (10^2+8^2)^{0.5})$ps, or ±28ps.

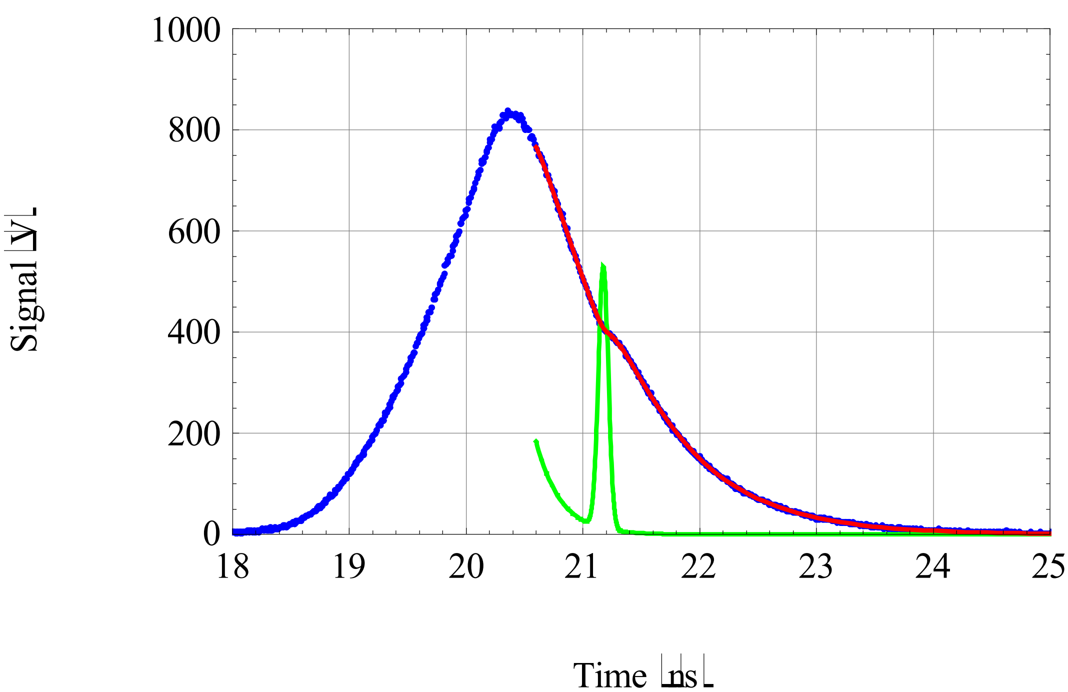

Figure 6. Recovered X-ray temporal profile (green) from a fit (red) to synthetic capsule plus hohlraum data (blue). We estimate ~30ps total error in X-ray bang-time measurement, corresponding to ±1eV or 1.5% in soft X-ray drive.

7. Conclusions

A new diagnostic for measuring X-ray bang-time for ICF ignition capsule implosions has been developed. The instrument will be fielded on the NIF and will deliver X-ray bang-time measurements with ±30ps precision, corresponding to +/- 1eV or 1.5% soft X-ray drive. This capability is realized even in the presence of substantial LPI induced bremsstrahlung and thermal background radiation using a HOPG monochromating crystal to select the X-ray band from the capsule with maximum contrast against background components. Shielding against direct radiation from the hohlraum and indirect radiation from the chamber wall and other secondary sources is provided by a thick hevimet enclosure and inner bulkheads.

Acknowledgments

The authors wish to acknowledge the staff of the Jupiter Laser Facility at LLNL for their support during the testing phase of the instrument on the Comet laser. This work was performed under the auspices of the U.S. Department of Energy by Lawrence Livermore National Laboratory under Contract No. DE-AC52-07NA27344 (Authorization Review No. LLNL-JRNL-XXXXXX)

References

[1] *J. D. Lindl et al., The physics basis for ignition using indirect-drive targets on the National Ignition Facility, Phys. Plasmas* ***11*** *(2004) 339*

[2]*G.B. Zimmerman et al., Numerical simulation of laser initiated fusion, Comments Plasma Phys. Controlled Fusion* ***2*** *(1975) 51*

[3] *M. M. Marinak et al., Three-dimensional HYDRA simulations of National Ignition Facility targets, Phys. Plasmas* ***8*** *(2001) 2275*

[4] *O. Landen et al., Capsule performance optimization in the National Ignition Campaign, Phys. Plasmas* ***17*** *(2010) 056301*

[5] *N. B. Meezan, et al., National Ignition Campaign hohlraum energetics, Phys. Plasmas* ***17*** *(2010) 056304*

[6] *V. Yu. Glebov et al., Prototypes of National Ignition Facility neutron time-of-flight detectors tested on OMEGA, RSI* ***75*** *(2004) 3559*

[7] *V. Yu. Glebov et al., High-yield bang time detector for the OMEGA laser, Rev. Sci. Instrum. 77 (2006) E712*

[8] *S.H. Glenzer et al., Symmetric Inertial ConfinementFusion Implosions at Ultra-High Laser Energies, Science* ***327*** *(2010) 1228*

[9] *M.B. Schneider et al., Images of the laser entrance hole from the static x-ray imager at NIF, Rev. Sci. Instrum.* ***81*** *(2010) E538*

[10]*C. Cerjan, Lawrence Livermore National Laboratory, Private communication.*

[11] *E.L. Dewald et al., Hot electron measurements in ignition relevant Hohlraums on the National Ignition Facility, Rev. Sci. Instrum.* ***81*** *(2010) D938*

[12] *G.A. Kyrala, Measuring symmetry of implosions in cryogenic Hohlraums at the NIF using gated x-ray detectors (invited), Rev. Sci. Instrum.* ***81*** *(2010) 10E316; and B.A. Hammel et al., Diagnosing and controlling mix in NIF imoplosian experiments, submitted to Phys. Plasmas (Nov 2010)*

[13] *N. Izumi, Lawrence Livermore National Laboratory, Private communication.*

[14] *T. Döppner et al., High order reflectivity of highly oriented pyrolytic graphite crystals for x-ray energies up to 22 keV, Rev. Sci. Instrum.* ***79*** *(2008) E311*

[15] *A. Pak,et al., X-ray line measurements with high efficiency Bragg crystals, Rev. Sci. Instrum.* ***75*** *(2004) 3747*

[16] *J. A. Halbleib et al., ITS: the integrated TIGER series of electron/photon transport codes-Version 3.0, IEEE Trans. Nucl. Sci.* ***39*** *(1992) 1025*
[17] *Greenfield Technology, 9 rue des Sablons, 91650 Breuillet, France*
[18] *O. S. Jones, Lawrence Livermore National Laboratory, Private communication.*